



**New Technology for Microfabrication and Testing
of a Thermoelectric Device for Generating Mobile
Electrical Power**

**by Patrick J. Taylor, Nibir K. Dhar,
Brian Morgan, and Bruce Geil**

ARL-TR-4480

June 2008

NOTICES

Disclaimers

The findings in this report are not to be construed as an official Department of the Army position unless so designated by other authorized documents.

Citation of manufacturer's or trade names does not constitute an official endorsement or approval of the use thereof.

Destroy this report when it is no longer needed. Do not return it to the originator.

Army Research Laboratory

Adelphi, MD 20783-1197

ARL-TR-4480

June 2008

New Technology for Microfabrication and Testing of a Thermoelectric Device for Generating Mobile Electrical Power

Patrick J. Taylor, Brian Morgan, and Bruce Geil
Sensors and Electron Devices Directorate, ARL

Nibir Dhar
DARPA MTO

REPORT DOCUMENTATION PAGE

*Form Approved
OMB No. 0704-0188*

Public reporting burden for this collection of information is estimated to average 1 hour per response, including the time for reviewing instructions, searching existing data sources, gathering and maintaining the data needed, and completing and reviewing the collection information. Send comments regarding this burden estimate or any other aspect of this collection of information, including suggestions for reducing the burden, to Department of Defense, Washington Headquarters Services, Directorate for Information Operations and Reports (0704-0188), 1215 Jefferson Davis Highway, Suite 1204, Arlington, VA 22202-4302. Respondents should be aware that notwithstanding any other provision of law, no person shall be subject to any penalty for failing to comply with a collection of information if it does not display a currently valid OMB control number.

PLEASE DO NOT RETURN YOUR FORM TO THE ABOVE ADDRESS.

1. REPORT DATE (DD-MM-YYYY) June 2008		2. REPORT TYPE		3. DATES COVERED (From - To)	
4. TITLE AND SUBTITLE New Technology for Microfabrication and Testing of a Thermoelectric Device for Generating Mobile Electrical Power				5a. CONTRACT NUMBER	
				5b. GRANT NUMBER	
				5c. PROGRAM ELEMENT NUMBER	
6. AUTHOR(S) Patrick J. Taylor, Nibir K. Dhar, Brian Morgan, and Bruce Geil				5d. PROJECT NUMBER	
				5e. TASK NUMBER	
				5f. WORK UNIT NUMBER	
7. PERFORMING ORGANIZATION NAME(S) AND ADDRESS(ES) U.S. Army Research Laboratory ATTN: AMSRD-ARL-SE-EI 2800 Powder Mill Road Adelphi, MD 20783-1128				8. PERFORMING ORGANIZATION REPORT NUMBER ARL-TR-4480	
9. SPONSORING/MONITORING AGENCY NAME(S) AND ADDRESS(ES)				10. SPONSOR/MONITOR'S ACRONYM(S)	
				11. SPONSOR/MONITOR'S REPORT NUMBER(S)	
12. DISTRIBUTION/AVAILABILITY STATEMENT Approved for public release; distribution unlimited.					
13. SUPPLEMENTARY NOTES					
14. ABSTRACT We report the results of the fabrication and testing of a thermoelectric power generation module. The module was fabricated using a new "flip-chip" module assembly technique that is scalable, modular, and results in a low value of contact resistivity ($\leq 10^5 \Omega\text{-cm}^2$). It can be used to leverage new advances in thin-film and nanostructured materials for the fabrication of new miniature thermoelectric devices. It may also enable monolithic integration of large devices or tandem arrays of devices on flexible or curved surfaces. Under mild testing, a power of 22 mW/cm ² was obtained from small (<100 K) temperature differences. At higher, more realistic temperature differences, ~500 K, where the efficiency of these materials greatly improves, this power density would scale to between 0.5 and 1 W/cm ² . These results highlight the excellent potential for the generation and scavenging of electrical power of practical and usable magnitude for remote military applications using thermoelectric power generation technologies.					
15. SUBJECT TERMS Thermoelectric, electrical power generation, flip-chip bonding					
16. Security Classification of:			17. LIMITATION OF ABSTRACT	18. NUMBER OF PAGES	19a. NAME OF RESPONSIBLE PERSON Patrick J. Taylor
a. REPORT U	b. ABSTRACT U	c. THIS PAGE U			19b. TELEPHONE NUMBER (Include area code) (301) 394-1475

Contents

List of Figures	iv
List of Tables	iv
Introduction	1
Experimental	2
Materials characterization	2
Assembly	2
Results	3
Device characteristics	3
Elevated Temperature Testing:.....	4
Discussion	5
Toward Realistic Applications	5
Path Towards Chip-Level Assembly	6
Significance	7
Summary and Conclusions	8
References	9
Distribution List	10

List of Figures

Figure 1. (a) Break-out view of the individual components, (b) view of the separate hot- and cold-junctions, and (c) the final device after flip-chip assembly	3
Figure 2. The output power density from the flip-chip module over the ΔT 100 K range.....	5
Figure 3. Flip-chip hybridizer used to bond devices at the chip and component level.....	7

List of Tables

Table 1. Measured properties of the components prior to assembly.	2
------------------------------------------------------------------------	---

Introduction

Although the efficiency of thermoelectric (TE) power generation is generally considered low, there are many military needs for electrical power that TE technologies can uniquely and successfully address. TE power generation has exceptionally rich potential to contribute to electrical power generation scavenged from waste heat and, hence, improve fuel utilization on vehicles. TE power generation modules can be tandem-connected in series which may also help expand the range of the power spectrum to ranges where there is current need: 100's of Watts. Because TE power generators can be miniaturized to integrated circuit/MEMS sizes, there are unique light-weight applications for mounted and dismounted Soldier power such as remote power for sensors, power for autonomous microsystems/robotics, and portable/wearable power for Soldiers.

Several attractive features of TE technology include no moving parts, light-weight, modularity, covertness, silence, high power density, low amortized cost, and long service life with no required maintenance. Many of the potential uses for mounted/dismounted power, such as recharging batteries, are therefore ideal for TE technologies. However, these applications will require interconnected, smaller-scale modular devices than are currently available. Most commercial off the shelf (COTS) TE devices are optimized for cooling, not for generating power, so new device structures with materials and geometries better optimized for power generation are needed for broader use of TE technologies.

Therefore, the goal of this work was to investigate new miniaturization and fabrication techniques to enable new military capabilities that can exploit recent developments in materials with improved ZT , or index of power conversion efficiency. Using the results of this work, the development of low-cost adaptable fabrication where power generators can be directly integrated with miniature autonomous microsystems, or with curved exhaust systems on vehicles, is sought. An additional objective is to develop an understanding of the potential for generating usable electrical power from myriad adventitious heat sources for these and other new military applications.

To reduce the number of variables of this work, we have chosen to study well-known materials with good efficiency in TE power generators that we recognize can be miniaturized. N-type PbTe and p-type Sb_2Te_3 were identified for this initial device, with longer-term interest in alternate materials whose thermal conductivity may be reduced by incorporating nanostructures (*1 through 3*) or electrical properties could be improved with quantum-confinement heterostructures (*4*). Although PbTe and Sb_2Te_3 are generally much more efficient at higher temperatures, they are suitable for showing that in this quite moderate temperature range, the new miniaturization concepts are highly effective for the military applications of interest.

Experimental

Materials Characterization

The PbTe and Sb₂Te₃ TE legs were polished to a specular finish to reduce uncertainty in geometry and thus, reduce measurement error. Each sample had similar geometries: 0.40 cm in length, 0.25 cm in width, and 0.10 cm in depth (5). All geometrical dimensions were measured using a micrometer thickness gauge which yields measurements that are accurate to about 2%. The TE properties measured for these materials are summarized in table 1 where ρ is the electrical resistivity, α is the Seebeck coefficient, and κ is the thermal conductivity (6).

Table 1. Measured properties of the components prior to assembly.

	ρ ($\times 10^{-3} \Omega\text{cm}$)	α ($\times 10^6 \text{ V/K}$)	κ ($\times 10^{-3} \text{ W/cm K}$)	Doping ($/\text{cm}^3$)	Mobility ($\text{cm}^2/\text{V sec}$)
PbTe	0.5	-96.5	32.9	1×10^{19}	1075
Sb₂Te₃	0.6	+124.6	22.0	6×10^{19}	185

Assembly

The metal junctions of the device were fabricated from oxygen-free copper stock so that the contribution to the total electrical resistivity from the hot and cold junctions is negligible. Further, the thermal conductivity is significantly better in copper than either of the semiconductors, so the junctions remain isothermal. To maintain permanent electrical isolation between the different sections of the TE module, the metal junctions were mounted on a thin square aluminum nitride (AlN) platen having an area of 6.25 cm².

The components are shown in figure 1 at the various stages of assembly. In figure 1a, the large copper heat-sink, the AlN top isolation with serpentine trace, one of the metal junctions (positioned next to the copper heat-sink), and one of the Sb₂Te₃ components (positioned next to the length scale) are shown. In figure 1b, the PbTe and Sb₂Te₃ components are shown fully integrated with copper hot-junctions permanently mounted to the top AlN isolator. Between that and the length scale are the three copper cold-junctions permanently mounted onto the bottom AlN isolator. To proceed with the “flip-chip” assembly, a special mechanical x-y translation stage was designed to accurately manipulate and strategically position the hot-junction onto the cold junctions permanently mounted onto the copper heat sink. Once in position, the metallurgical junctions were formed by application of pressure and heat. Fabricated in this way, the obtained device shown in figure 1c is mechanically rugged and fully operational.

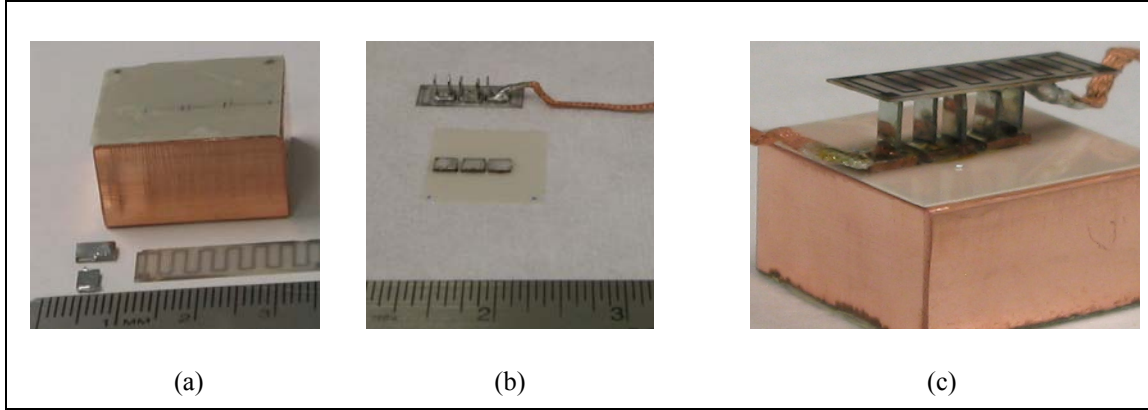


Figure 1. (a) Break-out view of the individual components, (b) view of the separate hot- and cold-junctions, and (c) the final device after flip-chip assembly

Results

Device Characteristics

The initial characteristics of the device were determined immediately after assembly. The device's total electrical resistance was experimentally found to be 0.432Ω and remained stable throughout thermal testing. The resistivity of the oxygen-free copper is $1.7 \times 10^{-6} \Omega\text{-cm}$, so the contribution to the total device resistance from the sum of the resistance from all six copper junctions is more than almost five orders of magnitude less than that from the semiconductor materials, so the dominant contributions would be only from the semiconductors, and potentially from the average contact resistance, R_c . The theoretical resistance of the device (R_d) can be calculated using equation 1, using the measured resistivity (ρ) values from independent Hall effect measurements listed in table 1 and the cross-sectional area (A) and length (l) for each of the individual "i" components along with each of the "j" contacts according to:

$$R_d = \sum_j (R_c)_j + \sum_i \rho_i \left(\frac{l_i}{A_i} \right) \quad (1)$$

R_d for this device is 0.432Ω , which is consistent with the experimental value. Because the theoretical and experimental resistance values are consistent to three significant figures, R_c must be $10^{-5} \Omega\text{-cm}^2$ or lower. The agreement between experimental and calculated R_d is likely fortuitous, in part, because of the relative uncertainty from the geometry measurement, believed to be about 2%. However, the fact that the measured and predicted values are obtained as the average of $j = \text{ten}$ separate contacts highlights the fact that each contact must have excellent integrity and that the assembly technique is highly effective, robust, and practical.

For higher temperature tests, the device was mounted in a vacuum system to prevent oxidation of the materials and reduce error from convective heat flow. Two type-K thermocouples were used to independently determine the temperature hot-junction at the top of the device and a third thermocouple was used to measure the temperature of the cold-junction on the large heat sink on the bottom.

Elevated Temperature Testing

To test the device for power generation, the hot-junction was heated radiatively by a 30 W “HotWatt” electrical power resistor. The resistor was not in contact with the TE device so as to minimize thermal mass. The output power was measured from the two braided copper terminals shown in figure 1c. To assure that the device had reached a steady-state temperature difference, the range of temperature difference was slowly scanned from $\Delta T = 0$ to 100 K. To normalize this electrical power to the area from which it was generated, we calculated the cross-sectional area of all the elements of the device and determined the power density which is plotted as a function of temperature difference in figure 2.

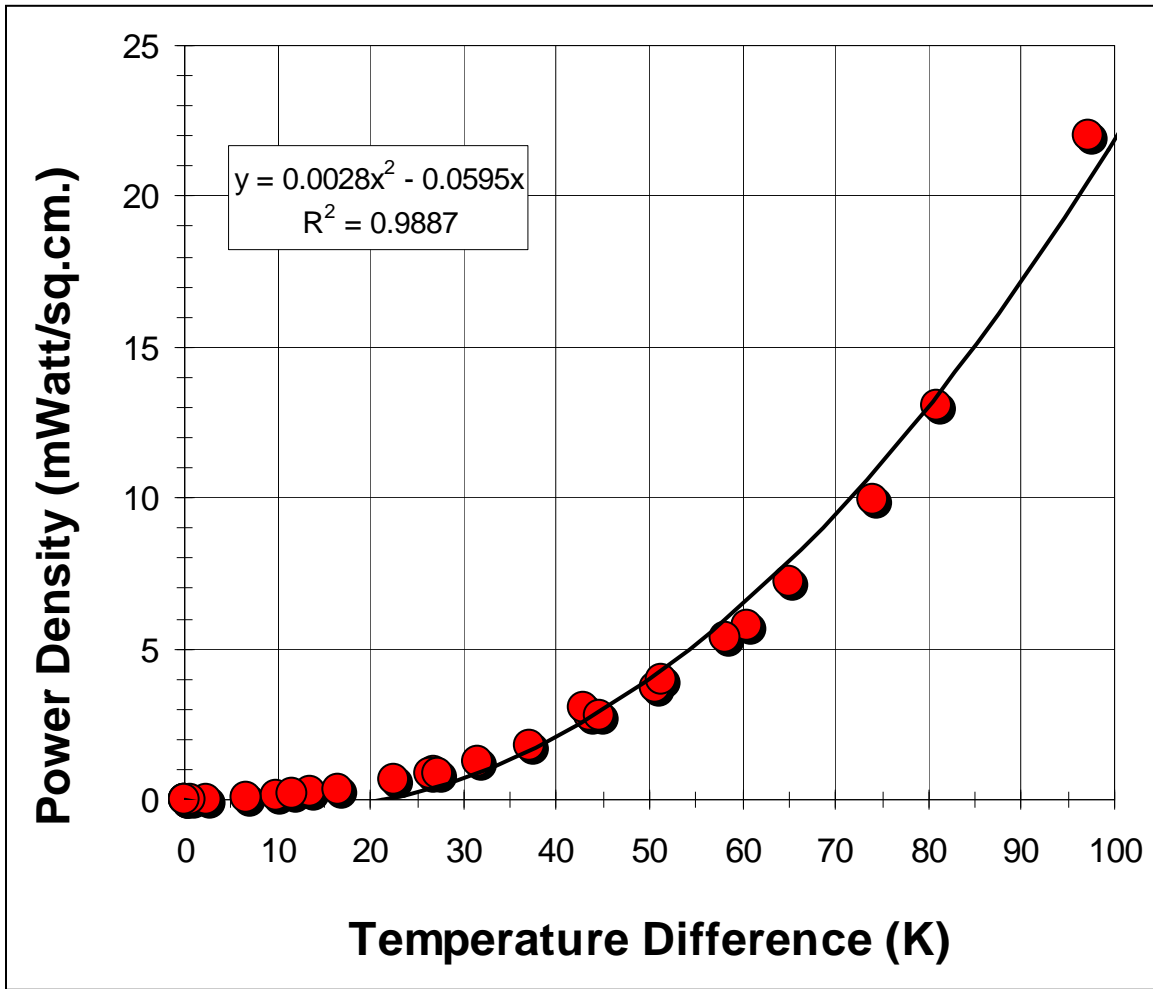


Figure 2. The output power density from the flip-chip module over the ΔT 100 K range.

Discussion

Toward Realistic Applications

Although this device is not perfectly impedance-matched, its performance under thermal testing is excellent and can be used to qualify its potential for power generation in more realistic applications. One application could be to provide electrical power from the waste heat energy from vehicles that would otherwise be dissipated and lost to the environment. In such a power-scavenging role, we can assume the temperature difference between some heated engine component and the ambient environmental temperature (ΔT) ranges between 400 and 500 K. The output power density of the device (P) will increase as a function of the square of the

temperature difference, ΔT^2 . Analytically fitting the obtained experimental data from this study to such a quadratic form yields the relation given in equation 2:

$$P = \left[(2.8 \times 10^{-3})(\Delta T^2) - (5.95 \times 10^{-2})(\Delta T) \right] \quad (2)$$

The correlation coefficient for the fit between the data and the analytical fit is 0.9887 which provides good confidence. However, the extra term that is linearly dependent on ΔT likely results from parasitic heat losses, from the change in the properties (e.g., resistivity) with temperature and other phenomena assumed to be constant in this analysis.

Extrapolated to the 400-500 K temperature difference range, this expression predicts that this device would provide power densities between 0.5 W/cm^2 and 1 W/cm^2 . Since the TE properties of these materials dramatically increase at higher temperature, that extrapolation is conservative. Because of that, it is believed that the TE output power density would exceed 1 W/cm^2 .

This extrapolation would hold for the condition of a hard, fixed ΔT . If the experimental measurement were conducted under a finite heat load where the flow of heat through the device results in a decrease in ΔT across it, this extrapolation would necessarily decrease somewhat. For instance, if the thickness were 0.2 cm instead of 0.1, the electrical resistance and thermal resistance both scale with area and decrease by a factor of 2. The temperature difference would therefore decrease because of the additional thermal “drain”. The absolute power could actually decrease by a factor of 2, meaning that the power-per-area calculation would be a factor of four smaller. However, because in this test we have assumed a fixed ΔT , the heat flux would double so the area and resistance changes would cancel and the power-per-area calculation would remain consistent.

Regardless, even over the mild 100 K temperature difference shown in this demonstration, $22 \text{ milliWatts/cm}^2$ is a particularly attractive value for power density and shows TE power generation from waste heat would find wide use and application for military applications in the field such as power for small battlefield electronics, portable power, and recharging batteries.

Path Towards Chip-Level Assembly

The high power density also points to the utility of this new fabrication technology for producing even more highly miniaturized and integrated, state-of-the-art power sources. Because this new fabrication assembly yields low contact resistance, it can be scaled to microscopic dimensional scales consistent with integrated circuits (IC's) and micro-electromechanical systems (MEMS). Such a demonstration would show excellent potential for providing power for autonomous microsystems, robotics and portable/wearable power for mounted/dismounted units.

IC and chip-level integration of TE power components can be accomplished using special flip-chip hybridization equipment as shown in figure 3. Using such equipment for massive TE array

fabrication would represent new enabling technology for next-generation, very highly-integrated TE power generation device technology.

This new approach would represent one path toward leveraging attractive, new record-high TE results from thin film research for potentially disruptive new technologies for TE power generation.

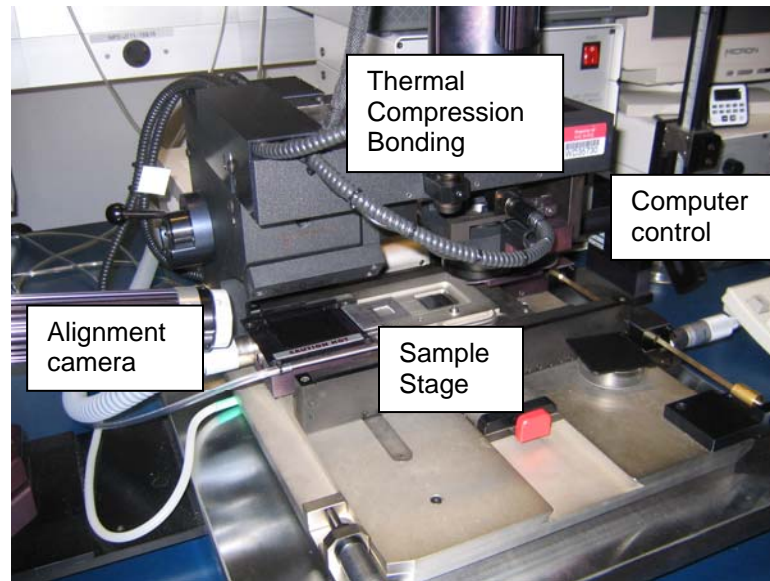


Figure 3. Flip-chip hybridizer used to bond devices at the chip and component level.

Significance

In this work, we have shown one path towards new fabrication of micro-scale TE power generating devices. The fabrication results in successful operation and provides very low resistance contacts consistent with state-of-the-art soldering/hand assembly. Highly-integrated, smaller scale TE device arrays having massive row-by-column arrays are possible. However, they cannot be assembled by soldering, hand assembly, or pick-and-place techniques. The number of TE devices per array would range on the order of 10^6 and larger. Flip-chip assembly could be modified to be used to fabricate larger scale devices where the module may have to be integrated onto a curved surface.

Summary and Conclusions

In this work, the results of the fabrication and testing of a TE power generation module show attractive potential for new TE device technology using a new “flip-chip” module assembly. Flip-chip assembly is scalable, modular, and in this work we have shown low value of total internal electrical resistance and a contact resistivity of $\leq 10^5 \Omega\text{-cm}^2$. It is also one path to leverage new advances in thin-film and nanostructured materials for the fabrication of new miniature TE devices, or those on non-planar curved surfaces. In series connection of many TE device arrays, the power output could be scaled to 100's of Watts. For the prototype device of this work, under mild testing, a power of 22 mW/cm^2 was obtained from small ($<100 \text{ K}$) temperature differences. At higher, more realistic temperature differences, $\sim 500 \text{ K}$, where the efficiency of these materials greatly improves, this power density would scale to between 0.5 and 1 W/cm^2 . These results highlight the excellent potential for the generation and scavenging of electrical power of practical and usable magnitude for remote military applications using TE power generation technologies.

References

1. Venkatasubramanian, R.; Siivola, E.; Colpitts T.; O'Quinn, B. Thin-film thermoelectric devices with high room-temperature figures of merit. *Nature* **2001**, *413*, 597–602.
2. Harman, T. C.; Taylor, P. J.; Walsh, M. P.; LaFoge, B. E. Quantum Dot Superlattice Thermoelectric Materials and Devices. *Science* **2002**, *297*. (5590) 2229.(2002).
3. Hogan, T.; Downey , A.; Short, J.; D';Angelo, J.; Wu, C.; Quarez, E.; Androulakis, J.; Poudeu, P.; Sootsman, J.; Chung, D.; Kanatzidis, M.; Mahanti, S. D.; Timm, E.; Schock, H.; Schock, Ren, F.; Johnson, J.; Case, E. Nanostructured Thermoelectric Materials and High-Efficiency Power-Generation Modules. *Journ. of Elect. Mat.* **2007**, *36* (7), 704.
4. Hicks. L.; Dresselhaus, M. Effect of quantum-well structures on the thermoelectric figure of merit. *Phys. Rev. B* **47** **1993**, 12727.
5. To obtain fully optimum TE performance, the geometry ratios of the PbTe and the Sb₂Te₃ should be adjusted so that each component is perfectly impedance matched to each other. While this condition probably does not apply perfectly to the device of this work, it is believed to be reasonably close and future devices are currently being designed that are more optimally impedance matched.
6. The thermal conductivity was calculated using the Wiedemann-Franz law and the measured values of electrical resistivity, the lattice thermal conductivity and known values for the Lorentz number.

<u>No. of Copies</u>	<u>Organization</u>	<u>No. of Copies</u>	<u>Organization</u>
1 (ELECT COPY	ADMNSTR DEFNS TECHL INFO CTR ATTN DTIC OCP 8725 JOHN J KINGMAN RD STE 0944 FT BELVOIR VA 22060-6218	1	ARMY RESEARCH OFFICE ATTN AMSRD ARL RO EL W CLARK III PO BOX 12211 RESEARCH TTRIANGLE PARK NC 27709
1	DARPA ATTN IXO S WELBY 3701 N FAIRFAX DR ARLINGTON VA 22203-1714	1	US ARMY TRADOC BATTLE LAB INTEGRATION & TECHL DIRCTR ATTN ATCD B 10 WHISTLER LANE FT MONROE VA 23651-5850
1	DARPA DSO ATTN S BEERMAN-CURTIN 3701 NORTH FAIRFAX DR ARLINGTON VA 22203-1714	1	US ARMY INFO SYS ENGRG CMND ATTN AMSEL IE TD F JENIA FT HUACHUCA AZ 85613-5300
1	DARPA MTO ATTN N DHAR 3701 NORTH FAIRFAX DR ARLINGTON VA 22203-1714	1	US ARMY RDECOM ATTN AMSRD AMR W C MCCORKLE 5400 FOWLER RD REDSTONE ARSENAL AL 35898-5000
1 CD	OFC OF THE SECY OF DEFNS ATTN ODDRE (R&AT) THE PENTAGON WASHINGTON DC 20301-3080	2	US ARMY RDECOM CERDEC ATTN AMSRD CER C2 AP ES C BOLTON ATTN AMSRD CER C2 AP ES S COOMBES 10125 GRATOIT RD STE 100 FT BELVOIR VA 22060
1	OFFICE OF NAVAL RESEARCH ONR HEADQUARTERS ATTN CODE 332 M GROSS 875 N RANDOLPH ST ARLINGTON VA 22203	1	US ARMY RSRCH LAB ATTN AMSRD ARL CI OK TP TECHL LIB T LANDFRIED BLDG 4600 ABERDEEN PROVING GROUND MD 21005-5066
1	US ARMY RSRCH DEV AND ENGRG CMND ARMAMENT RSRCH DEV AND ENGRG CTR ARMAMENT J MATTS BLDG 305 ABERDEEN PROVING GROUND MD 21005-5001	1	AIR FORCE RESEARCH LABORATORY ATTN AFRL/RXBT D DUBIS 2941 HOBSON WAY BLDG 654 RM 210 WRIGHT PATTERSON AFB OH 45433

<u>No. of Copies</u>	<u>Organization</u>
1	US GOVERNMENT PRINT OFF DEPOSITORY RECEIVING SECTION ATTN MAIL STOP IDAD J TATE 732 NORTH CAPITOL ST NW WASHINGTON DC 20402
1	US ARMY RSRCH OFC ATTN AMSRD ARL RO EM J PRATER PO BOX 12211 RESEARCH TRIANGLE PARK NC 27709-2211
18	US ARMY RSRCH LAB ATTN AMSRD ARL CI OK T TECHL PUB ATTN AMSRD ARL CI OK TL TECHL LIB ATTN AMSRD ARL SE D E SHAFFER ATTN AMSRD ARL SE DP J HOPKINS ATTN AMSRD ARL SE E G WOOD ATTN AMSRD ARL SE EM P UPPAL ATTN AMSRD ARL SE R P AMIRTHARAJ ATTN AMSRD ARL SE RL M DUBEY ATTN AMSRD ARL SE DP B GEIL ATTN AMSRD ARL SE DP B MORGAN ATTN AMSRD ARL SE DP N JANKOWSKI ATTN AMSRD ARL SE EI P TAYLOR (5 COPIES) ATTN AMSRD ARL SE EI P WIJEWAMASURIYA ATTN IMNE ALC IMS MAIL & RECORDS MGMT ADELPHI MD 20783-1197
Total:	35 (33 HCs, 1 Elect, 1 CD)

INTENTIONALLY LEFT BLANK